background level up to at least 10 MHz in the electric component.

The same wave measurements are also shown in the color spectrograms in Fig. 3a, together with other measurements made under different plasma conditions. Figure 3b shows results of measurements made when the beam was emitted along the magnetic field to within a few degrees. There is a net increase of the wave intensity up to 10 MHz in the electric component. In addition, narrow harmonics of the electron gyrofrequency are excited, as seen in both the electric and magnetic components.

Figure 3c shows the effect of operating the SEPAC electron beam accelerator (5 kV, 0.3 A). The beam was on continuously for 5 seconds. Several narrowband emissions are observed up to several times $f_C$. In Fig. 3d, which was recorded during another SEPAC electron beam accelerator operation, the effect of the magneto-plasma dynamic arcjet is clearly visible, about 300 msec after the start of the beam pulse, in both the electric and magnetic components.

*Conclusion.* The electron beams injected from the Spacelab pallet produced very clear effects. There were large variations of the shuttle-Spacelab potential with respect to the ambient plasma potential. The relaxation time of the vehicle potential with respect to the plasma potential after the beam is switched off varied from a few milliseconds up to several seconds, the latter result being unexpected. The electrical properties of the materials composing the surface of the spacecraft play an important role, which must be understood before the beam effects can be analyzed. The electron beams also created several instabilities linked to the electron gyrofrequency and its harmonics, and to the plasma and the upper hybrid frequency. In most cases there was a net increase of the electric component of the background noise level in a wide frequency range up to 10 MHz.

C. BEGHIN
*Laboratoire de Physique et Chimie de l'Environnement, 45045 Orleans, France*
J. P. LEBRETON
*Space Science Department, European Space Agency, European Space Research and Technology Centre, 2200 AG Noordwijk, Netherlands*
B. N. MAEHLUM
J. TROIM, P. INGSOY
*Norwegian Defense Research Establishment, Kjeller, Norway*
J. L. MĪCHAU
*Laboratoire de Physique et Chimie de l'Environnement*

**References and Notes**

1. B. Grandal, Ed., *Artificial Particle Beams Utilised in Space Plasma Physics* (Plenum, New York, 1982).
2. C. Beghin, *ESA J.* **3** (No. 2), 123 (1979).
3. _____, in *Active Experiments in Space* (ESA SP-195, European Space Agency, Paris, 1983).
4. The ion accelerator functioned nominally during the first day of the mission until a failure occurred. Ion beam–induced effects will not be discussed in this report.
5. K. Wilhelm *et al.*, *Science* **225**, 186 (1984).
6. T. Obayashi *et al.*, *ibid.*, p. 195.
7. S. Mende *et al.*, *ibid.*, p. 191.
8. The success of this experiment resulted from the work of a number of participants in the PICPAB project. In particular, we thank F. X. Sene, P. Gille, B. Narheim, and U. Gercke, who worked enthusiastically during integrations, flight simulations, and the flight. We also thank Y. Arnal, J.-J. Berthelier, J.-Y. Delahaye, A. Gonfalone, D. Henry, D. Klinge, J. Lavergnat, F. Malerba, N. Overaas, M. Pirre, L. Pomathiod, M. Sylvain, J. F. Karczewski, P. Decreau, and J. M. Illiano. Fruitful discussions with A. Pedersen in the course of the data analysis are acknowledged. We thank the CNES, ESA, NASA, and ERNO personnel for their support during various phases of the project. In particular, we appreciate the support of the ESA Operations Team and the collaboration of the Plasma Physics Discipline Group in the Payload Operations Control Center before and during the mission.

27 March 1984; accepted 10 May 1984

## Atmospheric Emissions Photometric Imaging Experiment

Abstract. *The atmospheric emissions photometric imaging experiment was flown on Spacelab 1 to study faint natural and artificial atmospheric emission phenomena. The instrument imaged optical emission in the region 2000 to 7500 angstroms with a television system consisting of two optical channels, one wide-angle and one telephoto. A third optical channel imaged onto the photochathode of a microchannel plate photomultiplier tube that has 100 discrete anodes. A hand-held image intensifier camera with an objective grating permitted spectral analysis of the earth's airglow and the shuttle glow. Preliminary data show magnesium ion emission features in the lower ionosphere as well as the spacecraft glow spectrum.*

One of the scientific objectives of Spacelab 1 was the investigation of the near-earth environment, a region "filled" with space plasmas consisting of charged particles. Spacelab missions are ideally suited for active experiments to study the behavior of these near-earth space plasmas. An active experiment is one in which the environment is perturbed by an artificial stimulus such as a particle beam or a wave injection and the response of the environment is observed. The earth's natural plasma environment or an artificial stimulus interacting with the earth's atmosphere often produces an optical signature such as the aurora or the airglow. The atmospheric emissions photometric imaging (AEPI) experiment was developed to investigate these optical emission signatures from Spacelab.

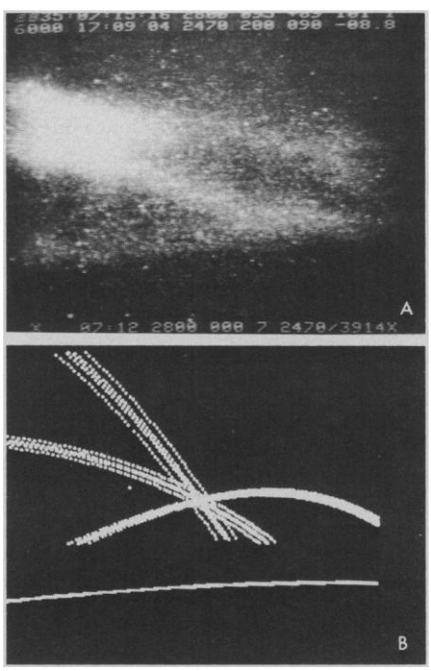


Fig. 1. (A) The 2800-Å filtered images taken by the AEPI television system on mission day 2 at 15 hours, 15 minutes (day 335, 07:15 UT). (B) Magnetic field line plots corresponding to 5 minutes before, during, and 5 minutes after the 2800-Å observations. Field lines are calculated at a distance of 1400 km in front of the observer. The times are: 335:07:10 UT (shallow plot up from left to right), 335:07:15 (shallow plot down from left to right), and 335:07:20 (steep plot down from left to right).

*Instrumentation.* The AEPI instrument (*1*) consists of a low-light-level television camera and an imaging photometer in a unit mounted on a two-axis pointing system located on the Spacelab pallet. It was controlled by a minicomputer and associated hardware located in the manned Spacelab module. The total mass of the AEPI experiment was 168 kg. Power consumption was typically 330 W. The AEPI instrument was developed jointly by Lockheed Missiles and Space Company and NASA–Marshall Space Flight Center with assistance from Boston College.

The sensing head of the AEPI instrument, the detector assembly, consists of two principal parts: a dual-channel, low-light-level television system (LLLTV) and a photon counting array (PCA). The system includes appropriate optical filters to provide spectral sensitivity and

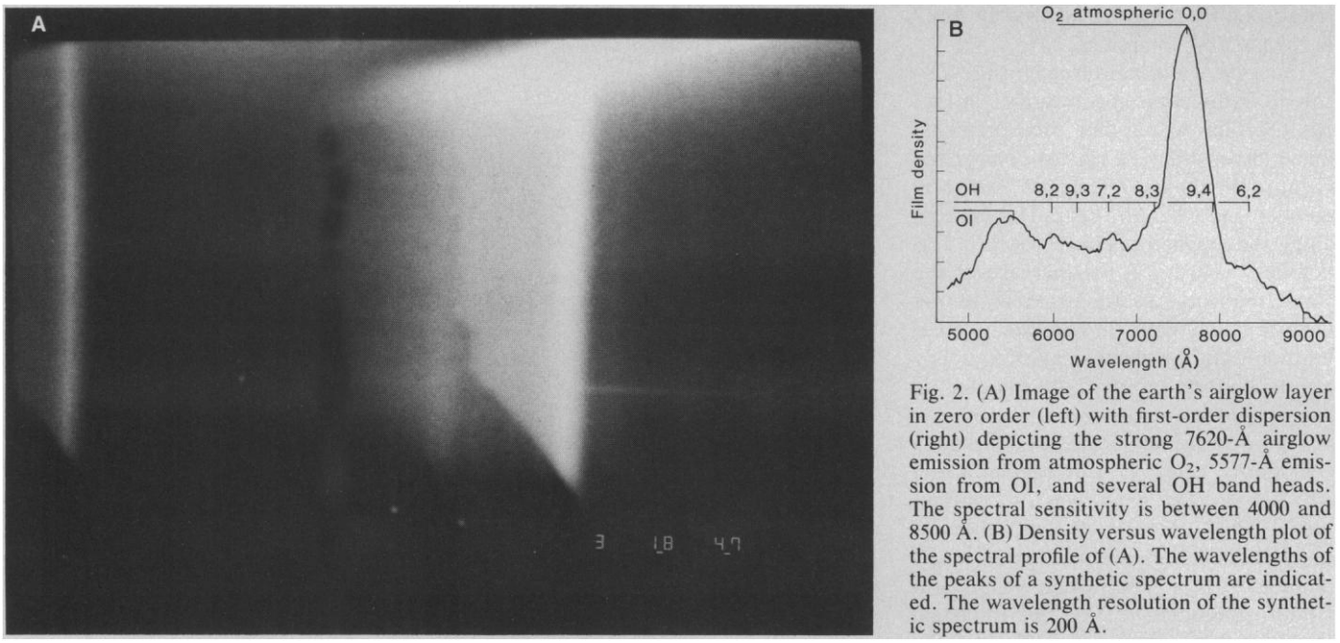


Fig. 2. (A) Image of the earth's airglow layer in zero order (left) with first-order dispersion (right) depicting the strong 7620-Å airglow emission from atmospheric $O_2$, 5577-Å emission from OI, and several OH band heads. The spectral sensitivity is between 4000 and 8500 Å. (B) Density versus wavelength plot of the spectral profile of (A). The wavelengths of the peaks of a synthetic spectrum are indicated. The wavelength resolution of the synthetic spectrum is 200 Å.

drive mechanisms and associated electronics to control filter wheels, focus the TV lenses, change the TV field of view, and effect PCA mode selection. The lens cover not only serves as a contamination cover and light baffle, but also houses light sources used to verify the sensitivity of the instrument in flight.

One of the TV channels has an *f*/2.0 lens with a 9.4-cm focal length and a nominal field of view of 20°. The design provides nearly parallel light through the interference filters, which ensures that the paraxial condition is satisfied for narrow-band filters. The lens elements are ultraviolet-transmitting fused silica, NaCl, or $CaF_2$. The other TV channel consists of an *f*/2.5, 2° × 3° telephoto lens with a 31.5-cm focal length, which is used to image with higher spatial resolution. A prism mounted in a movable carriage is used to select the field of view. Two filter wheels with five filter positions each accommodate a selection of eight interference filters.

The third optical system, the PCA, is boresighted with the LLLTV and contains an *f*/2.5, 2° × 3° telephoto lens of 23.9-cm focal length. The photocathode of a proximity-focused 100-anode microchannel plate photomultiplier tube forms the focal plane of the instrument. The output pulse current of the photomultiplier is proximity-focused on an array of 100 discrete anodes. The discrete anode array is a 10 by 10 matrix of anodes. With the multichannel plate operating at a gain of $10^6$ in the saturated node, the device counts photons from each anode. While crudely imaging, it is possible to obtain high-quality photometric data with this instrument. With the LLLTV and the PCA operating simultaneously, photometric intensities can be directly related to features in the TV image.

The AEPI instrument was controlled by the crew by means of the dedicated experiment processor (DEP) and the control panels located in the Spacelab module. The payload crew was assisted in instrument control by the personnel at the Program Operation Control Center (POCC) throughout the mission.

For photographing the atmospheric emission signatures near the vicinity of the shuttle, a "hand-held" image intensifier photographic camera was used. This type of camera was flown on previous shuttle flights STS-5 and STS-8 for the observation of the shuttle glow (*2–4*). This camera could be equipped with an objective grating or with seven different filters.

*Observations*. The basic scientific objective of the AEPI is the investigation of atmospheric radiation and optical contamination in the space shuttle environment. Many specific scientific objectives have been identified for the AEPI experiment on a series of Spacelab flights. A number of these objectives were accomplished on Spacelab 1 and some highlights of these AEPI observations are discussed in this report.

Ionospheric plasma is not observable optically from the ground because the ionospheric constituent species do not radiate in the visible region. However, sunlit magnesium ions can be detected in the ultraviolet because they radiate at 2800 Å due to resonance scattering of solar radiation. The detection and imaging of the magnesium ions provides an opportunity for the investigation of ionospheric processes. Photometric observations from satellites have shown that there should be an observable quantity of $Mg^+$ ions in the E and F regions of the ionosphere (*5–7*). One of the objectives of the AEPI experiment was to obtain images of ionospheric $Mg^+$ ion clouds.

An example of the AEPI $Mg^+$ observations is the image obtained on mission day 2 at 15 hours, 15 minutes. The orbiter was crossing the equator in the shadow traveling southeast. The position of the orbiter was latitude 3.1°, longitude 165.5°W, and altitude 252.7 km. The solar elevation angle according to the orbit predictions was −34.5°; that is, the orbiter was some 20° in the shadow. Looking out in the direction of the portside wing of the orbiter, the AEPI television instrument observed the scene shown in Fig. 1A through the 2800-Å (20-Å bandwidth) filter.

Figure 1A is a photograph of the AEPI television monitor. The alphanumeric characters displayed on the monitor at the top and bottom denote housekeeping parameters such as Universal time (UT), orbiter position, selected filters, camera operating parameters, and temperatures. The black region at the bottom is the dark earth. This is clearly distinguished as a curved boundary tilting slightly down toward the left. Above this boundary the atmosphere appears to show some bright features. Toward the top left, there is a luminous bright high-altitude cloud with two distinct fingers reaching out toward the bottom right with a low inclination angle. Since we assume that the cloud is sunlit ionized magnesium, these fingers should be aligned with the magnetic field.

The attitude of the vehicle was pitch 0°, yaw 180°, and roll −10°. That is, the orbiter was flying with the bay pointing away from the earth, the tail forward, and the port wing tilted down 10° so that the limb was in the AEPI field of view. The attitude was selected so that the AEPI instrument could make these earth limb observations.

A ground support software routine devised before the mission allowed the computation of the earth's magnetic field lines in the vicinity of the orbiter. The computer was tied into an image memory so that the position of the calculated field lines could be displayed on a TV monitor. This enabled us to display the apparent position of a set of magnetic field lines in the vicinity of the orbiter. Figure 1B shows the computed field line plots corresponding to the AEPI television field of view 5 minutes before, during, and 5 minutes after the observation of the equatorial magnesium ions. For each set, five field lines were plotted. The first field line was selected to go through a point located on the line of sight corresponding to the center of the picture, that is, located on the system's optic axis. This point is at a distance $D$ in front of the optical system. For Fig. 1B, $D$ was 1400 km, which gave the best match between the shape of magnetic field line and the observed $Mg^+$ fingers. For each set, the central field lines go through this point. The field lines were plotted as points at every 10 km from 100 km altitude up. This technique was used to illustrate the foreshortening of the field lines due to perspective effects. Besides the central field line, the four adjacent field lines in a set were selected by a fixed geographic latitude and longitude offset corresponding to a four-point square grid around the central field line.

Thus we can see that the observed magnesium striations are parallel to the magnetic field line located 1400 km from the orbiter. The selection of the field line defines the altitude of the center point of the image, which is 180 km for this case.

From these AEPI observations, it can be seen that imaging of the earth's ionosphere through the presence of the natural $Mg^+$ tracer ions is feasible. Quantitative analysis of this event and many other observations is in progress.

The hand-held image-intensifier camera permitted the observation of atmospheric airglow and of the glow associated with the shuttle. This camera could be operated in white light, in a filtered mode, or in a dispersion mode. In the dispersion mode, a diffraction grating was placed in front of the lens and the image produced was a result of diffraction through this objective grating.

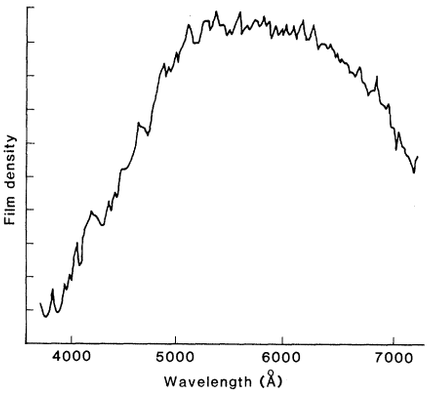


Fig. 3. Microdensitometer tracing of an image of spacecraft glow showing a structureless red glow.

The airglow spectrum in Fig. 2A shows a zero-order image of the earth's airglow layer on the left and first-order dispersion on the right. Note that the spacecraft orbital maneuvering system (OMS) pod indicates the airglow source at the lower right. The first spectral feature is a 5577-Å emission from atomic oxygen and the brightest feature is at 7620 Å. The 7620-Å feature was previously identified (*2*) as being the $O_2$ atmospheric bands. Figure 2B shows a microdensitometer tracing of the spectrum of Fig. 2A; the OH components were obtained from a 200-Å synthetic spectrum of vibrational transitions of OH (*8*).

A ram glow has been reported from earlier observations associated with the Atmospheric Explorer and Dynamic Explorer spacecraft (*9, 10*). The spatial distribution of the glow was observed from the orbiter vertical stabilizer as well as the OMS pod (*3*). Shown in Fig. 3 is a microdensitometer tracing of the spectrum of the spacecraft glow on the vertical stabilizer. Note that this tracing shows none of the structure that was seen in the airglow spectrum of Fig. 2B. It was suggested earlier (*11*) that OH might be a candidate species for producing the glow; however, it does not appear that OH plays a dominant part in the process resulting in the glow emission on the orbiter stabilizer.

The hand-held image intensifier camera was used to make many observations of the natural limb airglow layer. Because of the favorable transmission characteristics of the Spacelab view ports, the spectral observing regions could be extended farther toward the infrared. The naturally occurring OH Meinel bands were photographed in the airglow but were absent in similar photographs of the spacecraft glow. We are currently making a quantitative analysis of these types of images.

S. B. MENDE
*Lockheed Palo Alto Research Laboratory, Palo Alto, California 94304*
G. R. SWENSON
K. S. CLIFTON
*Space Science Laboratory, NASA–Marshall Space Flight Center, Huntsville, Alabama 35812*

**References and Notes**

1. W. G. Sandie, S. B. Mende, G. R. Swenson, M. E. Polites, *Opt. Eng.* **22**, 756 (1983).
2. S. B. Mende, P. M. Banks, R. Nobles, O. K. Garriott, J. Hoffman, *Geophys. Res. Lett.* **10**, 1108 (1983).
3. ———, *J. Spacecr. Rockets*, in press.
4. S. B. Mende, P. M. Banks, Da. A. Klingelsmith III, *Geophys. Res. Lett.* **11**, 527 (1984).
5. A. Boksenberg and J. C. Gerard, *J. Geophys. Res.* **76**, 4641 (1973).
6. J. C. Gerard, *ibid.*, **81**, 83 (1976).
7. ——— and A. Monfils, *ibid.* **83**, 4389 (1978).
8. S. Langhoff, personal communication.
9. J. H. Yee and V. J. Abreu, *Geophys. Res. Lett.* **10**, 126 (1983).
10. V. J. Abreu, W. R. Skinner, P. B. Hays, J. H. Yee, in *Proceedings of the AIAA Shuttle Environment and Operations Meeting* (AIAA, New York, 1983), p. 178.
11. T. G. Slanger, *Geophys. Res. Lett.* **10**, 130 (1983).
12. The flight of AEPI on Spacelab 1 was the result of the dedicated efforts of many people. We express our gratitude to all those at Lockheed Missile and Space Company and at Marshall Space Flight Center who were involved in the design and development of the AEPI instrument. We are also indebted to those who were involved in the integration and flight operations of Spacelab 1 at Marshall, Kennedy, and Johnson space centers. Special thanks are due to the crew of STS-9. The work at Lockheed was supported by NASA under contract NAS 8-32579.

27 March 1984; accepted 10 May 1984

## Isotopic Stack: Measurement of Heavy Cosmic Rays

Abstract. *A stack of plastic nuclear track detectors was exposed to heavy cosmic rays on the pallet of Spacelab 1. Some layers of the stack were rotated with respect to the main stack to determine the arrival time of the particles. After return of the stack the latent particle tracks are revealed by chemical etching. Under the optical microscope the charge, mass, energy, and impact direction of the particles can be deduced from the track geometry.*

*Experiment objectives.* Experiment 1ES024 on Spacelab 1 was designed to measure the chemical composition and energy spectra of heavy cosmic-ray nuclei with nuclear charge equal to or greater than 3. The exposure of a stack of nuclear track detectors on the Spacelab pallet allows the study of different